Optical Constants of Eyjafjallajökull Volcanic Ash: Analogs for Mars. T. L. Roush[1] A. Maturilli[2], J. Helbert[2], and H. Mannstein[3] [1]NASA Ames Research Center, MS 245-3, Moffett Field, CA 94035-1000, USA, [2]Institute for Planetary Research, DLR, Berlin, Germany, [3]Physics of the Atmosphere, DLR, Oberpfaffenhofen, Germany.

Introduction: There is ample evidence for wide spread volcanic ash on Mars [1, and references therein]. It is likely that the ash also occurs as a component of the atmospheric dust clouds [2-3 and references therein].

In the spring of 2010, the eruption of Eyjafjallajökull in Iceland may represent an analog of the volcanic activity that emplaced the ash deposits on Mars.

Quantitative modeling of the surface and atmospheric dust on Mars requires the optical constants of candidate materials [2-3 and references therein]. Here we describe our initial efforts at estimating the optical constants of various volcanic ash deposits associated with the Eyjafjallajökull eruption as analog materials for the materials on Mars.

Samples and Preparation: Ash samples were collected from a variety of locations. The sample for which we present initial results here was collected on the ground at Seljavellir ~8 km south of Eyjafjallajökull 2 months after the start of the main eruption. For the reflectance measurements, four grain size sieve fractions, 0-25, 25-63, 63-125, 125-250 µm, were created for each sample. Weber et al. [4] obtained in-flight elemental abundances of several aerosol particles during the eruption. These are compared to elemental abundances determined for soils on Mars [5-7] in Figure 1.

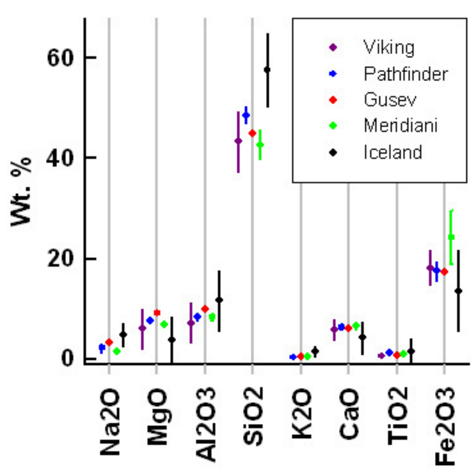

Figure 1. Weight percent oxide abundance of Icelandic aerosol particles compared to measurements of soils on Mars.

Laboratory Measurements: The Planetary Emission Laboratory at the DLR in Berlin [PEL, 8-9] is equipped with a Bruker Vertex 80V FTIR and an older Bruker IFS 88 For this study, we obtained reflectance measurements from 0.45 to 16µm using measurements from the IFS 88 for the short wavelength and the VERTEX 80V for the long wavelength. The measurements were joined at 1.1µm, where the spectral coverage of the both instruments overlap. An example of a series of measurements for one particle size fraction of one sample is shown in Figure 2.

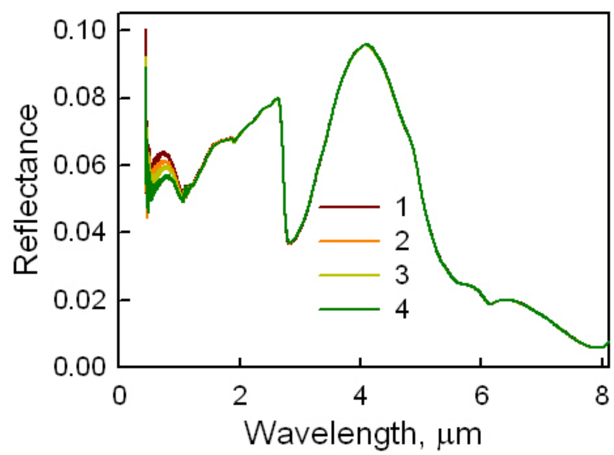

Figure 2. Reflectance of the Seljavellir 125-250 µm grain size sample repeated four times with a 10 minute delay.

Estimating Optical constants: The approach uses reflectance measurements of multiple grain sizes assuming the composition is constant [10]. An initial assumption is made regarding the wavelength behavior of the real index of refraction, *n*. A model of the interaction of light with particulate surfaces [11], as presented in [12] and [13], is used to determine the imaginary index, *k*, by iteratively calculating the reflectance and comparing the result to the measured reflectance using a χ^2-criterion. The interested reader is referred to [10] for more details. The median grain size of the sieve interval is used. Specifically for the 0-25, 25-63, 63-125, 125-250 µm samples we use 12.5, 44, 94, and 187.5 µm, respectively.

Here the internal scattering parameter is set to 0, isotropic scattering is assumed, and the width of the opposition surge is 0.05. The first parameter is poorly characterized for natural materials and setting it to zero effectively forces the absorption coefficient to account for all the spectral behavior. The last two parameters require observations at multiple viewing geometries that are not included in this initial effort.

A common assumption is that *n* is independent of wavelength [e.g. 14]. This is generally valid for the 0.4-2.5 µm region, but becomes increasingly incorrect at shorter and longer wavelengths. So we iterate the analyses by combining the initial, and subsequent, results via a subtractive Kramers-Konig (sKK) analysis to determine the wavelength dependence of *n* [10, 15-16]. For sKK one must define a value for the high frequency *n*. Here we use a value of 1.50 that is common for many silicate materials.

Initial results: Figure 3 shows the difference between successive iterations for both the *n* and *k*. The biggest change occurs when going from assuming *n* is constant (*n*0 and *k*0) to the next step where *n* is now a function of wavelength (*n*1 and *k*1). After four iterations, successive values of *n* (left column) and *k* (right column) are $<10^{-4}$ and $<10^{-5}$, respectively for all grain sizes. The final values of the *n* (left column) and *k* (right column) indices of refraction, derived for each grain size, are shown as the colored lines in the bottom panels of Fig 3. The mean and standard deviation of these values is shown as the gray points and associated one standard deviation error bars (note the points are so dense that this appears as a gray region for both indices). The variance observed in both indices is greater than the combined uncertainty in the measured reflectances. This is likely due to our assumptions regarding the grain size of each sieve fraction. However, without more detailed knowledge of the particle size distribution, we are unable to provide any tighter constraints on the resulting optical constants.

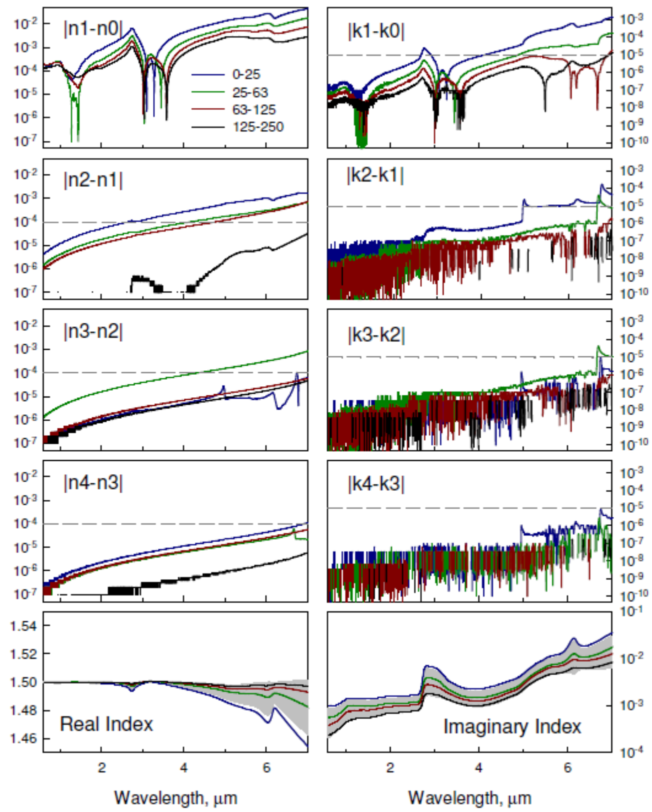

Figure 3. The successive change in the *n* (left column) and *k* (right column) indices of refraction. The terms n0 and k0 refer to the initial wavelength independent behavior of the *n* and associated *k* (top panels). At the bottom *n* and *k*, after the fourth iteration, are shown for each grain size. The gray area shows the mean and one standard deviation of these values.

References: [1] Kerber, L. et al. (2010) 41st *LPSC,* abst.# 1006. [2] Clancy et al. (1995) *JGR, 100*, 5251-5263. [3] Forget, F. (1998) *GRL, 25*, 1105-1108. [4] Weber, K. et al. (2011) *Atmos. Environ., in press*. [5] Bell, J.F. et al. (2000) *JGR-E, 105*, 1721-1755. [6] Gellert, R. et al. (2004) *Science, 305,* 829-832. [7] Rieder, R. et al. (2004) *Science, 306*, 1746-1749. [8] Maturilli, A. et al. (2006) *Plant. Sp. Sci. 54*, 1057-1064. [9] Maturilli, A. et al. (2008) *Planet. Sp. Sci., 56*, 420-425. [10] Roush, T.L. et al. (2007) *JGR-E, 112*, doi:10.1029/2007JE002920. [11] Hapke, B. (1993) *Theory of Reflectance and Emittance Spectroscopy*. Cambridge Univ. Press, New York. 455 pp. [12] Roush, T.L. (1994) *Icarus 108*, 243-254. [13] Cruikshank, D. et al. (1997) in *Pluto and Charon*, D.J. Tholen and A. Stern, Eds., University of Arizona Press, 221-267. [14] Lucey, P. (1998) *JGR 103*, 1703–1713. [15] Roush, T. (2003) *Meteor. Planet. Sci*. 38, 419-426. [16] Roush, T. (2005) *Icarus, 179*, 259-264.